DMD Fast Forward. Published on April 17, 2017 as DOI: 10.1124/dmd.117.075614
This article has not been copyedited and formatted. The final version may differ from this version.

Modeling Combined Immunosuppressive and Anti-inflammatory Effects of Dexamethasone and Naproxen in Rats Predicts the Steroid-Sparing Potential of Naproxen

Xiaonan Li, Debra C DuBois, Dawei Song, Richard R Almon, William J Jusko, Xijing Chen

Clinical Pharmacokinetics Laboratory, School of Basic Medicine and Clinical Pharmacy, China Pharmaceutical University, Nanjing, Jiangsu, 211198, China (XL, XC); Department of Pharmaceutical Sciences, School of Pharmacy and Pharmaceutical Sciences, State University of New York at Buffalo, Buffalo, NY, 14214, USA (XL, DCD, DS, RRA, WJJ); Department of Biological Sciences, State University of New York at Buffalo, Buffalo, NY, 14260, USA (DCD, RRA)

DMD Fast Forward. Published on April 17, 2017 as DOI: 10.1124/dmd.117.075614
This article has not been copyedited and formatted. The final version may differ from this version.

Running title: PK/PD of dexamethasone and naproxen in arthritis

Corresponding authors:

William J Jusko, Ph.D., Department of Pharmaceutical Sciences, School of Pharmacy and Pharmaceutical Sciences, State University of New York at Buffalo, Buffalo, NY, 14214, USA

Telephone: 716-645-2855, Fax: 716-829-6569, E-mail: wjjusko@buffalo.edu

Xijing Chen, Ph.D., Clinical Pharmacokinetics Laboratory, School of Basic Medicine and Clinical Pharmacy. China Pharmaceutical University, Nanjing, Jiangsu, 211198, China

Telephone: 86 25-83271286, Fax: 86 25-86185379, E-mail: chenxj-lab@hotmail.com

Number of text pages: 20

Number of tables: 5

Number of figures: 6

Number of references: 60

Number of words:

Abstract: 228

Introduction: 693

Discussion: 1480

ABBREVIATIONS:

CIA, collagen-induced arthritis; Con A, concanavalin A; CS, corticosteroids; COX, cyclooxygenase; CV%, coefficient of variation; DEX, dexamethasone; GR, glucocorticoid receptor; IP, intraperitoneal; IM, intramuscular; ISF, interstitial fluid; mPBPK, minimal physiologically based pharmacokinetic; NCA, non-compartmental analysis; NPX, naproxen; NSAIDs, nonsteroidal anti-inflammatory drugs; PBS, phosphate buffered saline; PD, pharmacodynamics; PK, pharmacokinetics; PG, prostaglandins; RA, rheumatoid arthritis; SF, synovial fluid; SC, subcutaneous; WBLP, whole blood lymphocyte proliferation.

DMD Fast Forward. Published on April 17, 2017 as DOI: 10.1124/dmd.117.075614
This article has not been copyedited and formatted. The final version may differ from this version.

ABSTRACT

Dexamethasone (DEX), a widely prescribed corticosteroid (CS), has long been the cornerstone for the treatment of inflammation and immunological dysfunctions in Rheumatoid Arthritis (RA). The CS are frequently used in combination with other anti-rheumatic agents such as nonsteroidal anti-inflammatory drugs (NSAIDs) and disease-modifying anti-rheumatic drugs (DMARDs) to mitigate disease symptoms and minimize unwanted effects. The steroid dose-sparing potential of the NSAID naproxen (NPX) was explored with *in vitro* and *in vivo* studies. We investigated the single and joint suppressive effects of DEX and NPX on the *in vitro* mitogen-induced proliferation of T lymphocytes in blood and their anti-inflammatory actions on paw edema in female and male Lewis rats with collagen-induced arthritis (CIA). DEX was far more potent than NPX in these systems as expected. Mathematical models incorporating an interaction term Ψ were applied to quantitatively assess the nature and intensity of pharmacodynamic (PD) interactions between DEX and NPX. Modest synergistic effects of the two drugs was found in suppressing the mitogenic response of T lymphocytes. A pharmacokinetic (PK)/PD/disease (DIS) progression model integrating dual drug inhibition quantitatively described the PK, time-course of single and joint anti-inflammatory effects (paw edema), and sex differences in CIA rats, and indicated additive effects of DEX and NPX. Further model simulations demonstrated the promising steroid-sparing potential of NPX in CIA rats, with beneficial effects of the combination therapy more likely in males than females.

DMD Fast Forward. Published on April 17, 2017 as DOI: 10.1124/dmd.117.075614
This article has not been copyedited and formatted. The final version may differ from this version.

Introduction

Rheumatoid arthritis (RA) is one of the most prevalent chronic inflammatory autoimmune diseases, causing pain, swelling and stiffness of joints, as well as cartilage destruction and bone erosion. It preferentially affects synovial tissues, but is also deleterious to other organ systems producing various systemic comorbidities. With the combination of a susceptible genetic background and environmental insults, a sequence of complex immune activation cascades are involved in the disease initiation and progression of RA (Smolen et al., 2016). In particular, active immune cells present in the synovial tissues, especially T-lymphocytes, play a key role in promoting the continuous autoimmune reactions by releasing various pro-inflammatory mediators such as cytokines and prostaglandins (PG) (Cavender et al., 1987; McInnes and Schett, 2011). Noticeable sex differences in the prevalence, disease course, and prognosis occur in RA, with females more affected (Jawaheer et al., 2006; van Vollenhoven, 2009). Conventional medications such as nonsteroidal anti-inflammatory drugs (NSAIDs) and corticosteroids (CS) remain first-line therapies for RA because of their rapid symptomatic effects compared to slower-acting disease-modifying anti-rheumatic drugs (DMARDs) and biological agents (Gaffo et al., 2006).

The CS have long been used for treatment of RA owing to their potent anti-inflammatory and immunosuppressive properties. They not only provide rapid control and improvement of inflammatory symptoms, but also exhibit disease-modifying effects (Kirwan, 1995). Dexamethasone (DEX) is one of the most frequently used therapeutic CS. As a synthetic glucocorticoid (GC), it acts primarily through binding to the cytosolic glucocorticoid receptor (GR) and causes inhibition of transcriptional factors such as nuclear factor kB (NF-kB) and activator protein-1 (AP-1), thus suppressing the activation of genes encoding various pro-inflammatory mediators that aggravate inflammation and cause tissue damage (Coutinho and Chapman, 2011). The rapid actions of DEX are partly ascribed to the non-genomic effects by directly regulating signal transduction pathways via membrane-associated GR and second messengers (Cato et al., 2002). Despite the significant therapeutic effects of DEX, its sustained use is limited by dose and

time-dependent adverse effects such as myopathy, growth retardation, metabolic disturbances, and osteoporosis (Saag et al., 1994). Owing to the chronic nature of RA, long-term steroid treatment remains common and necessary for alleviation of active disease activity. As a result, the undesired effects that are commonly associated with long-term and high dose steroid therapy have a profound influence on the health-related quality of life of RA patients.

The NSAIDs are widely prescribed drugs for their potent analgesic, antipyretic and anti-inflammatory properties. Their pharmacological effects are mainly attributed to inhibition of cyclooxygenase (COX) and the consequential decreased synthesis of pro-inflammatory PG, thereby reducing pain and inflammation and improving physical function (Ricciotti and FitzGerald, 2011; Crofford, 2013). Naproxen (NPX), a non-selective COX inhibitor, has been extensively used in the symptomatic management of RA. It shows balanced inhibitory potencies on both COX isoforms, constitutive COX-1 and inflammation-inducible COX-2 (Vane, 1971). NPX is better tolerated with respect to common adverse effects associated with NSAIDs (e.g. gastrointestinal bleeding and potential cardiovascular toxicity) compared to COX-selective NSAIDs (Lussier et al., 1978; Watson et al., 2002). However, like other NSAIDs, NPX is not disease modifying when used alone, thus providing the basis for its frequent use in combination therapy for RA.

Combination therapy has now become standard practice in treatment of RA. In view of the shared pharmacological effects of DEX and NPX in inhibiting the factors promoting disease production, we hypothesize that their joint use might permit dose reduction of DEX, thereby reducing side effects without compromising efficacy. The current work aims to assess the individual and joint pharmacodynamic (PD) effects of DEX and NPX through both *in vitro* and *in vivo* studies. Their combined immunosuppressive action was first evaluated by the *in vitro* inhibition of concanavalin A (Con A)-stimulated whole blood lymphocyte proliferation (WBLP). The pharmacokinetics (PK) of DEX in female and male healthy rats, the PK of NPX after co-administration of DEX, and the effects of NPX and DEX in collagen-induced arthritic (CIA) rats of both sexes were examined. Mathematical models incorporating a dual interaction equation were

DMD Fast Forward. Published on April 17, 2017 as DOI: 10.1124/dmd.117.075614
This article has not been copyedited and formatted. The final version may differ from this version.

applied to quantitatively describe the joint drug effects and the nature of drug interactions. Further model simulations were conducted to assess the potential degree of steroid dose-sparing effects of NPX.

Materials and Methods

Reagents and Chemicals. Pharmaceutical grade dexamethasone sodium phosphate solution was obtained from Bimeda Pharmaceuticals (Dublin, Ireland). Dexamethasone (purity > 98%), sodium naproxen, and concanavalin A (Con A) were purchased from Sigma-Aldrich Inc. (St Louis, MO). Dexamethasone-D5 (internal standard (IS), purity > 98%) was purchased from Toronto Research Chemicals Inc. (Toronto, Canada).The RPMI 1640 medium (Invitrogen; Grand Island, NY) was used for cell culture and serial dilutions of drugs in the WBLP assay.

Animals. Male and female Lewis rats (age 5-6 weeks), weighing approximately 110 g for females and 150 g for males, were purchased from Harlan (Indianapolis, IN). All rats were housed individually in the University Laboratory Animal Facility under controlled conditions with free access to water and food. Animals were acclimated for 1 week before experiments. These studies adhered to the Guide for the Care and Use of Laboratory Animals (Institute of Laboratory Animal Resources, 1996) and were approved by the University at Buffalo Institutional Animal Care and Use Committee.

Whole-Blood Lymphocyte Proliferation. The method detailed previously (Ferron and Jusko, 1998) was adapted with slight modifications. Briefly, blood (about 4 mL) from male healthy rats was collected into evacuated heparinized glass tubes and diluted 1:20 (v/v) with RPMI 1640 medium supplemented with 7.5% fetal calf serum, 100 U/mL penicillin, 100 μg/mL streptomycin, 2 mM L-glutamine, 20 mM HEPES and 0.25 mM 2-mercaptoethanol. Then 165 μL of the whole blood dilution was plated into each well of a flat bottom 96-well plate after adding 15 μL of mitogen (Con A; stock concentration 133 μg/mL in medium) and 20 μL of various concentrations of NPX and DEX alone or combined (Table 1). The cultures were incubated in a 5% CO_2-humidified incubator at 37°C for 72 h, then pulsed with 1 μCi of ^{3}H-thymidine per well (New England Nuclear, Boston, MA) and incubated for 18 h. The cells were harvested onto microplates (Packard Instrument Company), washed with 3% hydrogen peroxide, dried in an oven at 50°C for 2 h, mildly shaken on a plate shaker for 5 min after the addition of liquid scintillation fluid (Microscint-O,

Packard), and counted using a Top Count Microplate Scintillation Counter (Perkin Elmer, Waltham, MA).

Pharmacokinetics and Pharmacodynamics of DEX and NPX. The DEX dosing solution was freshly prepared by directly diluting the dexamethasone sodium phosphate solution (equivalent to 3 mg/mL DEX) with phosphate buffered saline (PBS). The NPX dosing solution was freshly prepared by dissolving sodium NPX into PBS (pH=8), and filtered through 0.22 micron filters before use. Both drugs were administered in a volume of 1 mL/kg.

The induction of CIA in the Lewis rats was conducted following procedures described previously (Earp et al., 2008b). Hind paw swelling was used to indicate edema and measured by digital calipers (VWR Scientific, Rochester, NY). After evaluation on day 15 for females and day 20 for males (one day before peak disease time), rats with a paw volume increase of at least 50% in one or two hind paws were selected and used in the subsequent PD study. For each sex group, the CIA rats were randomly divided into four subgroups (n=4): vehicle controls, which received only PBS intraperitoneally (IP); single drug groups, which received a bolus injection of either 55 mg/kg IP sodium NPX PBS solution (equivalent to 50 mg/kg NPX) or 0.225 mg/kg DEX subcutaneously (SC); and the combined group, which received 50 mg/kg IP NPX immediately after SC injection of 0.225 mg/kg DEX. All groups received injections on day 16 for females and day 21 for males post-disease induction. Paw edema was measured as the sum of the paw and ankle cross-sectional areas for each hind paw. Paw edema and body weights were monitored before disease induction (day 0) and post-induction 3, 7, 9, 10, 11, 13, 14, 15 days for both sex groups and 17 to 20 days for CIA males. Starting from the dosing day (day 16 for females and day 21 for males), paw edema was measured before dosing and at 1, 2, 4, 6, 8, 12, 24 and 36 h after dosing and on post-dose days 3, 4, 5, 6, 7, 8, 9 and 10. The paw volumes of 4 female and 4 male healthy rats were measured through the entire study to determine the natural growth.

The PK of SC DEX (2.25 mg/kg) was studied in female and male healthy rats. Serial blood samples were collected from the saphenous vein at post-dose 10, 20, 30 and 50 min and 1, 1.5,

2, 3, 4, 6, 8, 12, 24 h and processed and analyzed for DEX by a liquid chromatography-tandem mass spectrometry (LC-MS/MS) method used previously (Samtani and Jusko, 2007) with slight modifications. Briefly, 100 µL 4% phosphoric acid was added to 100 µL of plasma and then spiked with 10 µL of Internal Standard (IS) working solution. The mixture was vortex-mixed and centrifuged at 13000 ×*g* for 10 min at 10°C and then subjected to solid phase extraction. The dried residue was reconstituted with 200 µL acetonitrile-water (50:50, v/v) followed by vortexing and centrifugation at 13000 ×*g* for 10 min at 10°C. The supernatant was transferred into vials and used for LC-MS/MS injection. Chromatographic separations were achieved on a C8 Hydrobond AQ Column (particle size 3 µm, 150 × 2.1 mm; MAC-MOD Analytical Inc., Chadds Ford, PA) with the column oven temperature set at 30°C. The mobile phase consisted of eluent A (water containing 5 mM ammonium formate and 0.1% formic acid) and eluent B (acetonitrile/water (95:5 v/v) containing 1 mM ammonium formate and 0.1% formic acid) and was pumped at a flow rate of 0.2 mL/min with a gradient elution. The gradient profile was: 0 min, 40% B; a linear increase to 70% B from 0 to 2 min; 70% B for 3 min; a linear increase to 95% B over 0.1 min; 95% B for 1.9 min; a linear decrease to 40% B from 7 min to 7.1 min; 40% B for 3.9 min and stop at 11.0 min. The mass spectrometer was operated in the positive ionization mode for the detection of ion transitions at m/z 393.3/373.3 for DEX and 398.5/378.6 for IS. The system was controlled by Analyst software version 1.4 (Applied Biosystems SciEx, Toronto, Canada) for data acquisition and analysis.

The NPX concentrations in combined dosing groups were compared with those in single drug groups to assess the influence of single-dose DEX on the PK of NPX. Serial blood samples were collected from the saphenous vein at 15, 30 and 45 min and 1, 2, 4, 6, 9, 12, 24 h and analyzed for NPX by LC-MS/MS (Li et al. 2017a).

Linearity was found over the concentration ranges of 0.2 to 100 ng/mL for DEX and 0.125 to 40 µg/mL for NPX. For both bioanalytical assays, the coefficient of variation (CV%) of intra-

DMD Fast Forward. Published on April 17, 2017 as DOI: 10.1124/dmd.117.075614
This article has not been copyedited and formatted. The final version may differ from this version.

and inter-day accuracy and precision were less than 15%, and the recovery of the sample preparation method was around 90% for DEX and approached 100% for NPX.

Pharmacokinetic Models. The plasma concentration-time profiles of NPX were described by an extended minimal physiologically based pharmacokinetic (mPBPK) model with plasma and one tissue compartment (Figure 1). Detailed model descriptions and assumptions are provided in (Li et al, 2017b). The model equations and initial conditions are:

$$\frac{dA_{a,N}}{dt} = -k_{a,N} \cdot A_{a,N}\,, \qquad A_{a,N}(0) = \mathrm{Dose_N} \cdot F_N \tag{1}$$

$$\frac{dC_{p,N}}{dt} = \left[k_{a,N} \cdot A_{a,N} + f_{d,N} \cdot Q_{co} \cdot (C_{uISF,N} - C_{up}) - CL_{up} \cdot C_{up}\right]/V_p\,, \quad C_{p,N}(0) = 0 \tag{2}$$

$$\frac{dC_{ISF}}{dt} = \left[f_{d,N} \cdot Q_{co} \cdot (C_{up} - C_{uISF,N})\right]/V_{ISF}\,, \qquad C_{ISF}(0) = 0 \tag{3}$$

where $A_{a,N}$ indicates the amount of NPX at the absorption site, $k_{a,N}$ is the first-order absorption rate constant, $C_{p,N}$ and C_{ISF} are total NPX concentrations in V_p (plasma volume) and V_{ISF} (ISF volume), Q_{co} is cardiac plasma flow, $f_{d,N}$ is the fraction of drug in Q_{co} accessing V_{ISF}, CL_{up} is clearance of unbound NPX from plasma, C_{up} and $C_{uISF,N}$ are the unbound NPX concentrations in plasma and ISF that could be calculated from their corresponding total concentrations using the equations, albumin concentrations and binding parameters provided in (Li et al, 2017a, Li et al, 2017b), and F_N is the bioavailability of the IP dose calculated to be about 0.9 from literature-reported intravenous data in rats (Lauroba et al., 1986). The physiological restrictions of relevant parameters are:

$f_{d,N} \leq 1$ and $V_p + V_{ISF}$ = Extracellular Fluid Volume (ECF = 206.29 mL/kg) (Shah and Betts, 2012)

The plasma concentration-time profiles of DEX after 2.25 mg/kg SC injection to female and male healthy rats were characterized by the basic mPBPK model (Cao and Jusko, 2012) shown in Figure 1. The model equations and initial conditions describing DEX PK are:

$$\frac{dA_{a,D}}{dt} = -k_{a,D} \cdot A_{a,D}\,, \quad A_{a,D}\,(0) = \mathrm{Dose}_D \cdot F_D \tag{4}$$

DMD Fast Forward. Published on April 17, 2017 as DOI: 10.1124/dmd.117.075614
This article has not been copyedited and formatted. The final version may differ from this version.

$$\frac{dC_{p,D}}{dt} = \left[k_{a,D} \cdot A_{a,D} + f_{d,D} \cdot Q_{co} \cdot \left(\frac{C_t}{K_p} - C_{p,D} \right) - CL_p \cdot C_{p,D} \right] / V_p, \quad C_{p,D}(0) = 0 \tag{5}$$

$$\frac{dC_t}{dt} = \left[f_{d,D} \cdot Q_{co} \cdot (C_{p,D} - \frac{C_t}{K_p}) \right] / V_t \,, \quad C_t(0) = 0 \tag{6}$$

where $A_{a,D}$ is the amount of DEX at the absorption site, $k_{a,D}$ is the first-order absorption rate constant, $C_{p,D}$ and C_t are total DEX concentrations in V_p and V_t (tissue volume), K_p is tissue partition coefficient, $f_{d,D}$ is the fraction of drug in Q_{co} accessing V_t, CL_p is the systemic clearance, and F_{D} is the bioavailabilty of IM DEX (0.86) in rats (Samtani and Jusko, 2005; Earp et al., 2008c). The physiological restrictions of relevant parameters are:

$f_{d,D}$ ≤ 1 and V_p + V_t = Body weight

Several modeling assumptions were made for DEX: (1) Unbound DEX concentrations equilibrate rapidly between plasma, ISF and cell water; thus the free ISF DEX concentrations serve as the driving force for PD effects in CIA rats. (2) Protein binding of DEX is linear and occurs primarily to albumin in plasma (Cummings et al., 1990) and tissues with negligible binding to corticosteroid-binding globulin. (3) The binding of DEX to albumin in tissues occurs principally in the ISF. (4) The unbound fraction of DEX in plasma (f_{up}) is 0.3 for both sexes.

The unbound fraction of DEX in ISF (f_{uISF}) was calculated using :

$$f_{uISF} = \frac{1}{1+(E/P)(1-f_{up})/f_{up}} \tag{7}$$

where *E/P* is the ratio of protein concentrations in ISF and plasma with a value of 0.9 used for arthritic rats (McNamara et al., 1983, Li et al., 2017a).

The PK of DEX in rats was found to be linear with dose and not affected by RA (Samtani and Jusko, 2005; Earp et al., 2008c); therefore, the PK parameters obtained by fitting the PK data of 2.25 mg/kg of SC DEX in healthy rats were used to simulate the total tissue concentrations of DEX (C_t) in arthritic rats that received 0.225 mg/kg of SC DEX. The unbound DEX concentrations in ISF ($C_{uISF,D}$) were then generated from $C_{uISF,D} = C_t \cdot f_{uISF}$.

Pharmacodynamic Models

DMD Fast Forward. Published on April 17, 2017 as DOI: 10.1124/dmd.117.075614
This article has not been copyedited and formatted. The final version may differ from this version.

Single and Combined Drug Effects on Whole Blood Lymphocyte Proliferation. The drug effects on Con A-induced lymphocyte proliferation was evaluated by determining the incorporation of ^{3}H-thymidine into DNA, which is expressed as counts per minute (*CPM*). The inhibitory potency on lymphocyte proliferation of individual drug was described using

$$E = E_0 \cdot \left(1 - \frac{I_{max} \cdot C^{\gamma}}{IC_{50}{}^{\gamma} + C^{\gamma}}\right) \quad (8)$$

where E is the *CPM* in the presence of drug, E_0 is the baseline *CPM* in the absence of drug, I_{max} is the maximum effect achieved by either drug, IC_{50} is the drug concentration at 50% of maximum inhibition, C is the total concentration of NPX or DEX in the culture medium, and γ is the Hill coefficient for the immunosuppressive effect. All model parameters were fitted to the *CPM* values for each of the four wells of each drug concentration.

The combined inhibitory effects of the two drugs on lymphocyte proliferation were characterized by a joint interaction model (Chakraborty and Jusko, 2002). The published model was modified to allow for the estimation of actual *CPM* values instead of normalized *CPMs*.

$$E = E_0 \cdot \left[1 - \frac{\begin{array}{c} I_{max,N} \cdot \left(\frac{C_N}{IC_{50,\mathrm{N}}}\right)^{\gamma_N} + I_{max,D} \cdot \left(\frac{C_D}{(\varphi_1 \cdot IC_{50,\mathrm{D}})}\right)^{\gamma_D} \\ + \left(I_{max,N} + I_{max,D} - I_{max,N} \cdot I_{max,D}\right) \\ \times \left(\frac{C_N}{IC_{50,\mathrm{N}}}\right)^{\gamma_N} \cdot \left(\frac{C_D}{(\varphi_1 \cdot IC_{50,\mathrm{D}})}\right)^{\gamma_D} \end{array}}{\begin{array}{c} \left(\frac{C_N}{IC_{50,\mathrm{N}}}\right)^{\gamma_N} + \left(\frac{C_D}{(\varphi_1 \cdot IC_{50,\mathrm{D}})}\right)^{\gamma_D} \\ + \left(\frac{C_N}{IC_{50,\mathrm{N}}}\right)^{\gamma_N} \cdot \left(\frac{C_D}{(\varphi_1 \cdot IC_{50,\mathrm{D}})}\right)^{\gamma_D} + 1 \end{array}}\right] \quad (9)$$

where φ_1 is the interaction term for lymphocyte proliferation inhibition where values of 1 indicate no interaction, less than 1 synergism, and greater than 1 antagonism.

Single and Combined Drug Effects in Rat Arthritis. Figure 1 depicts a general model scheme for the entire arthritis progression with the anti-inflammatory effects of NPX and DEX acting on paw edema production. The PK/PD model structure for the single drug effects of NPX was presented in (Li et al. 2017b). In this model, we assumed that the paw size increase in healthy

DMD Fast Forward. Published on April 17, 2017 as DOI: 10.1124/dmd.117.075614
This article has not been copyedited and formatted. The final version may differ from this version.

rats follows logistic growth. Therefore, before disease onset the rate of change of the paw volume over time in all groups is:

$$\frac{dPaw}{dt} = k_g \cdot Paw \cdot \left(1 - \frac{Paw}{Paw_{ss}}\right),\ t < t_{onset} \quad Paw(0) = Paw^0 \tag{10}$$

where Paw is the sum of ankle and paw cross-sectional areas of a rat hind foot; Paw_{ss} is the normal paw size at steady-state, k_g is the natural first-order growth rate constant of paw in healthy rats, and t_{onset} is the time delay observed before disease onset.

After disease onset, the paw volume-time profiles in the control group with no drug are:

$$\frac{dPaw}{dt} = k_g \cdot Paw \cdot \left(1 - \frac{Paw}{Paw_{ss}}\right) + k_{in}\,(t)\ - k_{out} \cdot Paw,\ t \geq t_{onset} \quad Paw(0) = Paw^0 \tag{11}$$

$$\frac{dk_{in}}{dt} = -k_{deg} \cdot k_{in}, \qquad k_{in}(0) = k_{in}^0 \tag{12}$$

where $k_{in}\,(t)$ is a function of time and represents the production of paw edema after disease onset; k_{deg} is a linear decline in k_{in} accounting for the natural remission of arthritis; and k_{out} is the first-order rate constant describing the loss of edema.

Based on the mechanisms of drug action, indirect response model I (IDR I) was applied to describe the individual inhibitory effects of NPX and DEX on paw edema production (Dayneka et al, 1993). The rate of change of paw size over time for a single drug were described as:

$$\frac{dPaw}{dt} = k_g \cdot Paw \cdot \left(1 - \frac{Paw}{Paw_{ss}}\right) + k_{in}\,(t) \cdot \left(1 - \frac{I'_{max} \cdot C'}{IC'_{50} + C'}\right) - k_{out} \cdot Paw,\ t \geq t_{onset} \qquad Paw(0) = Paw^0 \tag{13}$$

where I'_{max} is the maximum inhibition effect of either NPX or DEX on production of paw edema and IC'_{50} is the unbound ISF concentration (C') of drug required for 50% of maximal effect.

The combination effects of NPX and DEX were characterized using a dual drug inhibition approach (Earp et al., 2004). The paw size change over time in combined treatment groups is:

$$\frac{dPaw}{dt} = k_g \cdot Paw \cdot \left(1 - \frac{Paw}{Paw_{ss}}\right) + k_{in}\,(t) \cdot \left(1 - \frac{I'_{max,N} \cdot C_{uISF,N}}{IC'_{50,N} + C_{uISF,N}}\right) \cdot \left(1 - \frac{I'_{max,D} \cdot C_{uISF,D}}{\varphi_2 \cdot IC'_{50,D} + C_{uISF,D}}\right) - k_{out} \cdot Paw, \qquad t \geq t_{onset} \qquad Paw(0) = Paw^0 \tag{14}$$

DMD Fast Forward. Published on April 17, 2017 as DOI: 10.1124/dmd.117.075614
This article has not been copyedited and formatted. The final version may differ from this version.

where Ψ_2 is the interaction term for inhibition of paw edema production as defined for Eq 9. The model assumes that the drugs inhibit the pro-inflammatory processes (k_{in}) as directly demonstrated for DEX by Earp et al (2008b). Values of I_{max} and IC_{50} for each drug were generated from their individual studies allowing Ψ_2 to be resolved from the studies with joint NPX and DEX administration.

Model Fitting and Data Analysis. Naïve-pooled data from all replicates in the WBLP assay were analyzed jointly. Initial non-compartmental analysis (NCA) of the PK data of NPX and DEX was performed using Phoenix WinNonlin 6.4 software (Certara Corporation, Princeton, NJ). All PK data for NPX from our previous study (Li et al., 2017a) and this study were fitted jointly as well as DEX PK data for both sexes. The obtained PK parameter estimates were fixed in the subsequent PD analysis in CIA rats. All model fittings involved nonlinear regression using the maximum likelihood algorithm in ADAPT 5 (Biomedical Simulations Resource, Los Angeles, CA) (D'Argenio et al., 2009). All model codes are provided in the Supplementary Data Files. The variance model was set as:

$$V_i = (\sigma_1 + \sigma_2 \cdot Y_i)^2 \quad (15)$$

where V_i represents the variance of the ith data point and Y_i is the ith model prediction and σ_1 and σ_2 are variance model parameters that were estimated together with other system parameters during model fitting. Model selection was based on the goodness-of-fit criteria which included Akaike Information Criterion (AIC), visual inspection of the fitted profiles, and CV% of the parameter estimates. Statistical analysis of PK parameters was performed using SPSS software version 22 (IBM SPSS Statistics, Chicago, IL), and $p < 0.05$ was considered to be statistically significant.

DMD Fast Forward. Published on April 17, 2017 as DOI: 10.1124/dmd.117.075614
This article has not been copyedited and formatted. The final version may differ from this version.

Results

Single and Combined Effects of DEX and NPX on Whole Blood Lymphocyte Proliferation. Profiles for single drug inhibition of lymphocyte proliferation are presented in Figure 2. Both drugs showed concentration-dependent inhibition of lymphocyte proliferation. The sigmoidal I_{max} model (Eq. 8) was able to well-capture the concentration-response relationships of the individual agents (See Supplemental model code for single drug effects in WBLP). The parameter estimates for single drugs as well as interaction parameters for both drugs and their precision are listed in Table 2. Both NPX and DEX produced complete suppression of cell proliferation and thus both I_{max} values were fixed to 1.0. The IC_{50} of NPX for WBLP was estimated to be 83.97 μg/mL, which is slightly lower than reported for human lymphocytes (350 μg/mL) (Panush, 1976). It is very close to the peak plasma concentration (79 μg/mL) achieved in RA patients after 500 mg twice daily doses of NPX (van den Ouweland et al., 1987). This is in accordance with previous findings that the anti-proliferative effects of NSAIDs often occur at doses/concentrations high enough to suppress inflammatory responses (Seng and Bayer, 1986). DEX was more efficacious in suppressing lymphocyte proliferation than NPX as indicated by the 5-fold difference in their log IC_{50} values. The estimated IC_{50} value of DEX (1.5 ng/mL) is comparable to that using human whole blood culture (3.8 ng/mL) (Mager et al., 2003), which suggests that the anti-proliferative effect and sensitivity of the mitogenic response of lymphocytes to DEX are similar across species. The Hill coefficient γ was 3.04 for DEX, similar to that for NPX (2.92). The fittings included baseline *CPM* values for complete assessment of all parameters with potential variability. The combination effects of NPX and DEX on lymphocyte proliferation was evaluated using 20 concentration combinations. These data were fitted using the joint interaction model (Eq. 9) where the interaction term Ψ was factored with the IC_{50} of DEX because the primary immunosuppressive effects were exerted by DEX. A three-dimensional surface plot (Figure 2C) shows the combined drug effects on lymphocyte proliferation, where the surface represents the model predictions using Eq. 9 based on the estimated parameters in Table 2 (See Supplemental

DMD Fast Forward. Published on April 17, 2017 as DOI: 10.1124/dmd.117.075614
This article has not been copyedited and formatted. The final version may differ from this version.

model code for combined drug effects in WBLP). The estimated Ψ_1 value was 0.94 (confidence interval 0.90-0.99), which is lower than 1. Therefore, the combination of NPX and DEX exhibits a slight synergistic effect on lymphocyte proliferation.

Pharmacokinetics of NPX and DEX in CIA Rats. The pharmacokinetics of NPX in the combined treatment groups was compared with that in the single drug groups from our previous study (Li et al., 2017a). The concentration-time profiles of NPX in CIA rats after giving 50 mg/kg NPX alone or together with 0.225 mg/kg DEX along with the model fittings and calculated total and unbound ISF NPX concentrations are illustrated in Figure 3. The NCA results for the primary PK parameters of NPX including area under the concentration-time curve (AUC), apparent clearance (*CL/F*), apparent volume of distribution (*V/F*), and terminal half-life ($t_{1/2}$) are listed in Table 3. No obvious visual differences are seen for the PK profiles and also no significant differences in the PK parameters was found, suggesting that single-dose DEX did not affect the PK of NPX in CIA rats. Therefore, the PK parameter estimates of NPX obtained using the extended mPBPK model with concentration-dependent protein binding in both plasma and ISF (Figure 1) from our previous study (Li et al., 2017b) (Table 4) were fixed and applied for the subsequent PD modeling.

The pharmacokinetics of DEX in female and male healthy rats receiving 2.25 mg/kg of SC DEX were assessed (Figure 4) and described by the basic mPBPK model with one tissue compartment shown in Figure 1 (See Supplemental model code for DEX PK estimation). The NCA results for the primary PK parameters of DEX indicates that the terminal half-life ($t_{1/2}$) of DEX is significantly shorter in males (Table 3), thus different clearance terms (CL_p) were assigned to female and male rats in the model. The mPBPK model was able to capture all the PK data of DEX in healthy rats quite well (Figure 4) and yielded precise parameter estimates with reasonable CV% values (Table 4). Plasma volume (V_p), tissue volume (V_t), and cardiac plasma flow (Q_{co}) are physiological parameters applicable to rats obtained from the literature (Shah and Betts, 2012), which were fixed in the model fitting. Absorption of DEX from the SC injection site was rapid with

DMD Fast Forward. Published on April 17, 2017 as DOI: 10.1124/dmd.117.075614
This article has not been copyedited and formatted. The final version may differ from this version.

a k_a value of 2.09 1/h, which is slightly smaller than that obtained after IM dosing (5.78 1/h) (Earp et al., 2008c). The male rats showed higher clearances ($CL_{p\ Males}$ = 197.7 mL/h/kg) than females ($CL_{p\ Females}$ = 137.8 mL/h/kg), consistent with the fact that DEX exhibits sex-specific metabolite profiles in rats where its microsomal metabolism is more rapid in males (Tomlinson et al., 1997). The estimated tissue partition coefficient (K_p) is 0.63, which is close to those calculated from the steady-state distribution volume (V_{ss}/BW = 0.7) and a literature-reported estimation method (0.5 for muscle) (Poulin and Theil, 2000). The fraction of cardiac plasma flow of DEX ($f_{d,D}$) was fixed to 1, consistent with rapid diffusion of DEX into tissues with blood flow-limited distribution. Model simulations (See Supplemental model code for DEX PK simulation) for tissue total and ISF unbound DEX concentrations in arthritic rats receiving 0.225 mg/kg of SC DEX are displayed in Figure 4 with the latter used as the driving force for PD effects of DEX.

Single and Combined Anti-inflammatory Effects of NPX and DEX. The PK/PD/DIS progression model displayed in Figure 1 quantitatively integrated the PK of NPX and DEX into the model for paw edema progression, where unbound ISF concentrations of NPX (Figure 3) and DEX (Figure 4) were used to drive their anti-inflammatory effects in arthritic rats (See Supplemental PK/PD/DIS progression model code). The model was applied to jointly fit the paw volume data from all groups with model fittings illustrated in Figure 5. The model simultaneously characterized the natural paw growth as well as progression of paw edema with or without treatments very well. All of the PD/DIS parameters were estimated quite precisely with reasonable CV% values (Table 5). The disease-specific parameter estimates for male arthritic rats are comparable to those reported previously (Earp et al., 2009; Lon et al., 2011).

In general, the paw edema RA progression of female and male arthritic rats in the present study showed similar patterns and trends with those obtained previously (Li et al, 2017b), where females exhibited higher incidences (80% *vs* 60%), earlier disease onset (t_{onset}, 258 *vs* 307 h), faster disease production rate (group-averaged k_{in0}, 2.02 *vs* 1.78 mm^2/h), and more severe symptoms. In the absence of drug, paw size changes over time before disease onset were

DMD Fast Forward. Published on April 17, 2017 as DOI: 10.1124/dmd.117.075614
This article has not been copyedited and formatted. The final version may differ from this version.

assumed to follow the logistic growth function (Eq. 11) and increased at the same rate as in healthy animals (the estimated k_g was 0.002 h^{-1} for both sexes).

The individual anti-inflammatory effects of NPX and DEX were characterized using Eq. 13. NPX was previously found to be more efficacious in male arthritic rats as demonstrated by the maximum inhibitory effect ($I'_{max,N}$, 1.0 *vs* 0.75 for females) and concentration for 50% maximal effect ($IC'_{50,N}$, 136 *vs* 221 ng/mL) (Li et al, 2017b). A pilot study assessing the effects of two single SC doses of DEX (0.225 and 2.25 mg/kg) on paw edema in female and male CIA rats was conducted (unpublished) and the paw edema data were described by the mPBPK/PD/DIS progression model (Figure 1) using unbound ISF DEX concentrations as the driving force for PD. Preliminary fittings revealed values of $I'_{max,D}$ that were 1.0 and thus it was set as 1.0 for both sexes. A lower $IC'_{50,D}$ value of 0.39 ng/mL obtained for males than females (0.62 ng/mL) (Table 5) suggested that DEX exhibited modestly stronger potency in males consistent with the effects of NPX. The strong inhibition of paw edema observed for the combined treatment groups was satisfactorily described by the mPBPK/PD/DIS progression model incorporating the joint interaction equation (Eq. 14). During the model fitting, all drug-specific PD parameters (I_{max} and IC_{50}) were fixed to the values listed in Table 5 with only the disease-specific parameters and interaction term Ψ_2 were estimated by simultaneously fitting all of the paw volume data from each sex group. The disease-related parameters were re-estimated to account for the between-batch variation of CIA animals. The interaction term Ψ_2 was found to be 1.16 (confidence interval 0.49-1.84) for females and 0.98 (0.25-1.71) for males, neither of which was significantly different from 1.0, indicating that the combination of the two drugs displays simple additive effects in both sex groups.

Simulation of Steroid-Sparing Effect of NPX in Arthritis. The PK/PD/DIS progression model well described all the paw volume data when fitted simultaneously with fixed values of certain drug-specific parameters and yielded quite reasonable parameter estimates. Therefore,

DMD Fast Forward. Published on April 17, 2017 as DOI: 10.1124/dmd.117.075614
This article has not been copyedited and formatted. The final version may differ from this version.

model simulations were performed based on the fitted parameters (Table 5) to compare the potential anti-inflammatory effects of different single doses of DEX and combinations with NPX on paw edema. This allowed us to evaluate the degree of potential steroid dose-sparing effects of NPX (i.e. Would giving NPX allow a substantially lower dose of DEX to be utilized to obtain equivalent efficacy to higher doses of DEX?). The same values of initial disease production rate constant (k_{in0}) and paw size on day 0 (Paw_0) were assigned to all groups in order to allow more intuitive comparisons of drug effects. The model-predicted paw edema-time profiles after concurrent administration of 50 mg/kg of NPX and 0.225 mg/kg of DEX, and various single doses of DEX (0.225, 2.25 and 22.5 mg/kg) are displayed in Figure 6. These simulations show that the combination therapy exhibits different degrees of steroid dose-sparing by NPX in female and male arthritic rats. Combined use of DEX (0.225 mg/kg) with NPX (50 mg/kg) was able to reduce paw edema to a similar extent as a 10-fold higher dose of DEX (2.25 mg/kg) for females and a 100-fold higher dose of DEX (22.5 mg/kg) for males.

DMD Fast Forward. Published on April 17, 2017 as DOI: 10.1124/dmd.117.075614
This article has not been copyedited and formatted. The final version may differ from this version.

Discussion

Corticosteroids have long been the mainstay of RA therapy owing to their potent immunosuppressive and anti-inflammatory actions. However, the clinical effectiveness of DEX and other CS is compromised by their long-term and dose-related adverse effects. We extended our previous PK/PD studies with NPX (Li et al, 2017a, 2017b) and DEX (Earp et al, 2008a, 2008b, 2008c) to investigate whether better therapeutic outcomes could be achievable by a combination of DEX and NPX and to ascertain whether sex differences exist.

First, the single and combined immunosuppressive actions of DEX and NPX were evaluated by the *In vitro* WBLP assay, which measures the mitogenic response of T lymphocytes to drugs. This assay is convenient to assess the nature and intensity of drug-drug interactions as it mimics the natural milieu and requires small blood volumes. The relative immunosuppressive potency of several therapeutic CS were studied previously using this assay (Mager et al., 2003). DEX inhibits T lymphocyte proliferation by suppressing NF-kB causing reduction of IL-2 gene expression, which is responsible for the proliferation and differentiation of T lymphocytes (Toribio et al., 1989). Insufficient attention has been paid to the immunologic actions of NSAIDs, although considerable evidence has shown their capability of suppressing lymphocyte activation (Kelly et al., 1979; Ali et al., 1984; Seng et al., 1990; Cicala et al., 2000). The commonly acknowledged mechanism of action of NSAIDs is to block the synthesis of PG via COX inhibition. However, PG were reported to inhibit the mitogen-induced proliferation of T cells (Goodwin et al., 1977). Therefore, the anti-proliferative effect of NSAIDs may involve COX-independent mechanisms. These drugs have been shown to inhibit DNA synthesis and cause cell growth arrest in the G1 phase (Bayer and Beaven, 1979). The nature and intensity of interactions between DEX and NPX on lymphocyte proliferation were evaluated. The slightly synergistic effect of NPX on the anti-proliferative action of DEX ($\Psi_1 < 1$) is promising in that combination therapy would add to and possibly potentiate the immunosuppressive activity of DEX.

To further examine the PD interactions between DEX and NPX, the joint anti-inflammatory effects of DEX and NPX was investigated *in vivo* using CIA rats, a well-established animal model that mirrors human RA (Holmdahl et al., 2001). Similar to humans, the CIA rat model exhibits consistent sex differences in the disease progression of arthritis in that females exhibit higher incidences, earlier disease onset, and worse symptoms. We used this animal model previously to assess the PK/PD of both NPX (Li et al., 2017b) and DEX (Earp et al., 2008a). NPX exhibited moderate but significant inhibitory effects on paw edema production in both sexes with slightly stronger efficacy in male rats, and DEX showed potent anti-inflammatory effects in male arthritic rats with 60% reduction of paw edema compared to untreated controls. In particular, DEX-dependent trans-repression of production of the cytokines TNF-α, IL-1β, and IL-6 plays a central role in the alleviation of paw edema and bone erosion in arthritic rats (Earp et al., 2008a).

Both female and male CIA rats were studied so that the influence of sex in the anti-inflammatory actions of DEX with NPX could be compared. The proposed PK/PD/DIS progression model (Figure 1) well characterized the anti-inflammatory effects of DEX and NPX both as single agents and in combination. The PK models include an extended mPBPK model with nonlinear binding for NPX adapted from our previous study (Li et al., 2017b) and a basic mPBPK model for DEX. The individual drug effects described by the inhibition model was linked to the calculated unbound ISF concentrations of both NPX and DEX. This was done for several reasons. As shown previously (Li et al., 2017b), the unbound NPX concentration-time profiles in ISF closely resembled those in synovial fluid (SF), which better correlate with the clinical efficacy of NPX as the synovium is the proposed site of action in RA (Jalava et al., 1977; Netter et al., 1989; Bertin et al., 1994; Day et al., 1995). DEX must permeate cells to bind to receptors and/or alter transcriptional factors, thereby exerting its effects. Rapid equilibration of unbound DEX concentrations between plasma, ISF, and cell water was thus assumed. According to their corresponding mechanisms of action, the joint effect of DEX and NPX was exerted on the

DMD Fast Forward. Published on April 17, 2017 as DOI: 10.1124/dmd.117.075614
This article has not been copyedited and formatted. The final version may differ from this version.

production process of paw edema in a joint and noncompetitive manner and therefore modeled using the dual drug inhibition approach (Chakraborty and Jusko, 2002; Earp et al., 2004).

The hepatic metabolism of NPX is mainly mediated by cytochrome P450 (CYP) 1A2 and 2C9 (Miners et al., 1996), which were reported to be induced by DEX *in vitro* (Gerbal-Chaloin et al., 2002; Vrzal et al., 2009). The NCA results for the primary PK parameters of NPX with or without joint dosing of DEX (Table 3) indicated that the single-dose of DEX had no significant influence on the PK of NPX in either female or male CIA rats. Previous studies have shown that the PK of DEX in CIA male rats was not altered by RA (Earp et al., 2008c) and DEX concentrations in healthy male rats after SC and IM dosing were shown to be identical (Earp et al., 2008a). The same situation was assumed here for female rats and thus DEX PK in healthy rats was used to model the PK in arthritic rats. In addition, the PK parameters after IM dosing of DEX in female rats were found to be in good agreement with those in males with 86% bioavailability for both sexes (Samtani and Jusko, 2005). We also assumed that the PK of DEX was not altered by NPX. Therefore, the same PK parameter values of DEX were applied for both single and combined drug groups. Male arthritic rats exhibited better responses to NPX, which can be partially explained by the higher unbound ISF concentrations of NPX (Li et al, 2017b). A similar sex-specific response was observed for DEX, consistent with previous findings that the anti-inflammatory actions of CS are more effective in males because they have more glucocorticoid-responsive genes (Duma et al., 2010). The IC_{50} values of NPX in both sexes are close to the peak unbound NPX concentrations in synovial fluid (SF) after a single dose of 500 mg NPX to arthritic patients (0.13 μg/mL) (Day et al., 1995), further confirming the feasibility of utilizing the unbound NPX concentrations in ISF/SF to mimic the biophase concentrations. In line with the *in vitro* results, DEX was more efficacious in reducing paw edema production in both sexes than NPX. For combination treatments in CIA rats, the interaction term Ψ_2 incorporated in the inhibition of paw edema production (Eq. 14) is similar to the Ψ_1 in Eq. 9, which reflects the magnitude by which the IC_{50} of DEX is altered by NPX. The estimated Ψ_2 values signified additive effects of combination

DMD Fast Forward. Published on April 17, 2017 as DOI: 10.1124/dmd.117.075614
This article has not been copyedited and formatted. The final version may differ from this version.

therapy in both sexes. Nevertheless, model simulations of the anti-inflammatory effects of various dosing regimens demonstrate promising steroid-sparing potential of NPX (Figure 6), especially for male arthritic rats. The occurrence of additivity is sufficient to produce steroid-sparing effects. The Ψ parameter is an empirical term that used to signify the nature of pharmacological interactions (synergic, additive or antagonistic) when detailed mechanisms are unclear. Further studies with the measurements of the molecular factors that drive chronic arthritis and that are relevant to the effects of DEX and NPX, such as the cytokines TNF-α, IL-1β, IL-6 and PGE_2, are necessary to better understand the sex-specific anti-inflammatory actions and the underlying mechanisms of interaction.

Overall, the drug-specific parameters (I_{max} and IC_{50}) of both drugs obtained *in vivo* were comparable to the *in vitro* values except that the maximum inhibition of NPX on paw edema in female arthritic rats was less than 1.0 (I_{max} = 0.75). This difference is quite reasonable since the whole blood used in the *in vitro* study was from healthy male rats and, more importantly, drug effects *in vivo* incur many additional complicating factors. In our study, the PD models were directly fitted to the actual measured *CPM* and pooled paw volume data without normalization by the control data, thus avoiding the impact of the variability from control groups (Woo et al., 2009).

In conclusion, the single and joint effects of DEX and NPX on the *in vitro* mitogen-stimulated proliferation of T lymphocytes and in assessing paw edema in female and male CIA rats were well described by mathematical models incorporating dual interaction equations for inhibition. With an interaction term Ψ, the proposed models also indicated the slight extent to which the potency (IC_{50}) of DEX is altered by NPX. Our study has thus mainly demonstrated additive immunosuppressive and anti-inflammatory effects of the drug combination. With the promising steroid-sparing potential of NPX, the combined use of DEX and NPX should permit dose reduction of steroids. The models may be useful to design preclinical studies with related drugs and devise clinical CS dosing regimens that maximize desired effects (immunosuppression and anti-inflammation) while minimizing unwanted effects in treatment of RA.

Authorship Contributions

Participated in research design: Li, DuBois, Song, Almon, Jusko, and Chen

Conducted experiments: Li, DuBois, and Song

Performed data analysis: Li, Song, and Jusko

Wrote or contributed to writing the manuscript: Li, DuBois, Song, Almon, Jusko, and Chen.

References

Ali AT, Hanson JM, and Morley J (1984) Effects of non-steroidal anti-inflammatory drugs on lymphocyte activation. *Agents Actions* **14:**216-222.

Ariens EJ, Van Rossum JM, and Simonis AM (1957) Affinity, intrinsic activity and drug interactions. *Pharmacol Rev* **9:**218-236.

Bayer BM and Beaven MA (1979) Evidence that indomethacin reversibly inhibits cell growth in the G1 phase of the cell cycle. *Biochem Pharmacol* **28:**441-443.

Bertin P, Lapicque F, Payan E, Rigaud M, Bailleul F, Jaeger S, Treves R, and Netter P (1994) Sodium naproxen: concentration and effect on inflammatory response mediators in human rheumatoid synovial fluid. *Eur J Clin Pharmacol* **46:**3-7.

Cao Y and Jusko WJ (2012) Applications of minimal physiologically-based pharmacokinetic models. *J Pharmacokinet Pharmacodyn* **39:**711-723.

Cato AC, Nestl A, and Mink S (2002) Rapid actions of steroid receptors in cellular signaling pathways. *Sci STKE* **2002:**re9.

Cavender D, Haskard D, Yu CL, Iguchi T, Miossec P, Oppenheimer-Marks N, and Ziff M (1987) Pathways to chronic inflammation in rheumatoid synovitis. *Fed Proc* **46:**113-117.

Chakraborty A and Jusko WJ (2002) Pharmacodynamic interaction of recombinant human interleukin-10 and prednisolone using in vitro whole blood lymphocyte proliferation. *J Pharm Sci* **91:**1334-1342.

Cicala C, Ianaro A, Fiorucci S, Calignano A, Bucci M, Gerli R, Santucci L, Wallace JL, and Cirino G (2000) NO-naproxen modulates inflammation, nociception and downregulates T cell response in rat Freund's adjuvant arthritis. *Br J Pharmacol* **130:**1399-1405.

Coutinho AE and Chapman KE (2011) The anti-inflammatory and immunosuppressive effects of glucocorticoids, recent developments and mechanistic insights. *Mol Cell Endocrinol* **335:**2-13.

Coxib, traditional NTC, Bhala N, Emberson J, Merhi A, Abramson S, Arber N, Baron JA, Bombardier C, Cannon C, Farkouh ME, FitzGerald GA, Goss P, Halls H, Hawk E, Hawkey C, Hennekens C, Hochberg M, Holland LE, Kearney PM, Laine L, Lanas A, Lance P, Laupacis A, Oates J, Patrono C, Schnitzer TJ, Solomon S, Tugwell P, Wilson K, Wittes J, and Baigent C (2013) Vascular and upper gastrointestinal effects of non-steroidal anti-inflammatory drugs: meta-analyses of individual participant data from randomised trials. *Lancet* **382:**769-779.

Crofford LJ (2013) Use of NSAIDs in treating patients with arthritis. *Arthritis Res Ther* **15 Suppl 3:**S2.

Cummings DM, Larijani GE, Conner DP, Ferguson RK, and Rocci ML, Jr. (1990) Characterization of dexamethasone binding in normal and uremic human serum. *DICP* **24:**229-231.

Day RO, Francis H, Vial J, Geisslinger G, and Williams KM (1995) Naproxen concentrations in plasma and synovial fluid and effects on prostanoid concentrations. *J Rheumatol* **22:**2295-2303.

D'Argenio D, Schumitzky, A, Wang, X. (2009) Adapt 5 User's Guide: Pharmacokinetic/Pharmacodynamic Systems Analysis Software, BMSR, University of Southern California.

Duma D, Collins JB, Chou JW, and Cidlowski JA (2010) Sexually dimorphic actions of glucocorticoids provide a link to inflammatory diseases with gender differences in prevalence. *Sci Signal* **3:**ra74.

Dayneka N, Garg V, and Jusko WJ, (1993) Comparison of Four Basic Models of Indirect Pharmacodynamic Responses, J. Pharmacokin. Biopharm., 21: 457-478.

Earp J, Krzyzanski W, Chakraborty A, Zamacona MK, and Jusko WJ (2004) Assessment of drug interactions relevant to pharmacodynamic indirect response models. *J Pharmacokinet Pharmacodyn* **31:**345-380.

Earp JC, Dubois DC, Almon RR, and Jusko WJ (2009) Quantitative dynamic models of arthritis progression in the rat. *Pharm Res* **26:**196-203.

Earp JC, Dubois DC, Molano DS, Pyszczynski NA, Almon RR, and Jusko WJ (2008a) Modeling corticosteroid effects in a rat model of rheumatoid arthritis II: mechanistic pharmacodynamic model for dexamethasone effects in Lewis rats with collagen-induced arthritis. *J Pharmacol Exp Ther* **326:**546-554.

Earp JC, Dubois DC, Molano DS, Pyszczynski NA, Keller CE, Almon RR, and Jusko WJ (2008b) Modeling corticosteroid effects in a rat model of rheumatoid arthritis I: mechanistic disease progression model for the time course of collagen-induced arthritis in Lewis rats. *J Pharmacol Exp Ther* **326:**532-545.

Earp JC, Pyszczynski NA, Molano DS, and Jusko WJ (2008c) Pharmacokinetics of dexamethasone in a rat model of rheumatoid arthritis. *Biopharm Drug Dispos* **29:**366-372.

Ferron GM and Jusko WJ (1998) Species- and gender-related differences in cyclosporine/prednisolone/sirolimus interactions in whole blood lymphocyte proliferation assays. *J Pharmacol Exp Ther* **286:**191-200.

Gaffo A, Saag KG, and Curtis JR (2006) Treatment of rheumatoid arthritis. *Am J Health Syst Pharm* **63:**2451-2465.

Gerbal-Chaloin S, Daujat M, Pascussi JM, Pichard-Garcia L, Vilarem MJ, and Maurel P (2002) Transcriptional regulation of CYP2C9 gene. Role of glucocorticoid receptor and constitutive androstane receptor. *J Biol Chem* **277:**209-217.

Goodwin JS, Bankhurst AD, and Messner RP (1977) Suppression of human T-cell mitogenesis by prostaglandin. Existence of a prostaglandin-producing suppressor cell. *J Exp Med* **146:**1719-1734.

Holmdahl R, Lorentzen JC, Lu S, Olofsson P, Wester L, Holmberg J, and Pettersson U (2001) Arthritis induced in rats with nonimmunogenic adjuvants as models for rheumatoid arthritis. *Immunol Rev* **184:**184-202.

Jalava S, Saarimaa H, Anttila M, and Sundquist H (1977) Naproxen concentrations in serum, synovial fluid, and synovium. *Scand J Rheumatol* **6:**155-157.

Jawaheer D, Lum RF, Gregersen PK, and Criswell LA (2006) Influence of male sex on disease phenotype in familial rheumatoid arthritis. *Arthritis Rheum* **54:**3087-3094.

Kelly JP, Johnson MC, and Parker CW (1979) Effect of inhibitors of arachidonic acid metabolism on mitogenesis in human lymphocytes: possible role of thromboxanes and products of the lipoxygenase pathway. *J Immunol* **122:**1563-1571.

Kirwan JR (1995) The effect of glucocorticoids on joint destruction in rheumatoid arthritis. The Arthritis and Rheumatism Council Low-Dose Glucocorticoid Study Group. *N Engl J Med* **333:**142-146.

Lanas A (2009) Nonsteroidal antiinflammatory drugs and cyclooxygenase inhibition in the gastrointestinal tract: a trip from peptic ulcer to colon cancer. *Am J Med Sci* **338:**96-106.

Lauroba J, Domenech J, Moreno J, and Pla-Delfina JM (1986) Relationships between biophasic disposition and pharmacokinetic behavior in nonsteroid antiinflammatory drugs. *Arzneimittelforschung* **36:**710-714.

Li X, DuBois DC, Almon RR, and Jusko WJ (2017a) Effect of disease-related changes in plasma albumin on the pharmacokinetics of naproxen in male and female arthritic rats, *Drug Metab Dispos*. Accepted for publication.

Li X, DuBois DC, Almon RR, and Jusko WJ (2017b) Modeling sex differences in pharmacokinetics, pharmacodynamics, and disease progression effects of naproxen in rats with collagen-induced arthritis, *Drug Metab Dispos*. Accepted for publication.

Lon HK, Liu D, Zhang Q, DuBois DC, Almon RR, and Jusko WJ (2011) Pharmacokinetic-pharmacodynamic disease progression model for effect of etanercept in Lewis rats with collagen-induced arthritis. *Pharm Res* **28:**1622-1630.

Lussier A, Arsenault A, and Varady J (1978) Gastrointestinal microbleeding after aspirin and naproxen. *Clin Pharmacol Ther* **23:**402-407.

Mager DE, Moledina N, and Jusko WJ (2003) Relative immunosuppressive potency of therapeutic corticosteroids measured by whole blood lymphocyte proliferation. *J Pharm Sci* **92:**1521-1525.

McInnes IB and Schett G (2011) The pathogenesis of rheumatoid arthritis. *N Engl J Med* **365:**2205-2219.

McNamara PJ, Gibaldi M, and Stoeckel K (1983) Fraction unbound in interstitial fluid. *J Pharm Sci* **72:**834-836.

Miners JO, Coulter S, Tukey RH, Veronese ME, and Birkett DJ (1996) Cytochromes P450, 1A2, and 2C9 are responsible for the human hepatic O-demethylation of R- and S-naproxen. *Biochem Pharmacol* **51:**1003-1008.

Netter P, Bannwarth B, and Royer-Morrot MJ (1989) Recent findings on the pharmacokinetics of non-steroidal anti-inflammatory drugs in synovial fluid. *Clin Pharmacokinet* **17:**145-162.

Panush RS (1976) Effects of certain antirheumatic drugs on normal human peripheral blood lymphocytes. Inhibition of mitogen- and antigen-stimulated incorporation of tritiated thymidine. *Arthritis Rheum* **19:**907-917.

Poulin P and Theil FP (2000) A priori prediction of tissue:plasma partition coefficients of drugs to facilitate the use of physiologically-based pharmacokinetic models in drug discovery. *J Pharm Sci* **89:**16-35.

Ricciotti E and FitzGerald GA (2011) Prostaglandins and inflammation. *Arterioscler Thromb Vasc Biol* **31:**986-1000.

Saag KG, Koehnke R, Caldwell JR, Brasington R, Burmeister LF, Zimmerman B, Kohler JA, and Furst DE (1994) Low dose long-term corticosteroid therapy in rheumatoid arthritis: an analysis of serious adverse events. *Am J Med* **96:**115-123.

Samtani MN and Jusko WJ (2005) Comparison of dexamethasone pharmacokinetics in female rats after intravenous and intramuscular administration. *Biopharm Drug Dispos* **26:**85-91.

Samtani MN and Jusko WJ (2007) Quantification of dexamethasone and corticosterone in rat biofluids and fetal tissue using highly sensitive analytical methods: assay validation and application to a pharmacokinetic study. *Biomed Chromatogr* **21:**585-597.

Seng GF and Bayer BM (1986) Inhibition of amino acid transport by nonsteroidal anti-inflammatory drugs: a model for predicting relative therapeutic potency. *J Pharmacol Exp Ther* **237:**496-503.

Seng GF, Benensohn J, and Bayer BM (1990) Changes in T and B lymphocyte proliferative responses in adjuvant-arthritic rats: antagonism by indomethacin. *Eur J Pharmacol* **178:**267-273.

Shah DK and Betts AM (2012) Towards a platform PBPK model to characterize the plasma and tissue disposition of monoclonal antibodies in preclinical species and human. *J Pharmacokinet Pharmacodyn* **39:**67-86.

Smolen JS, Aletaha D, and McInnes IB (2016) Rheumatoid arthritis. *Lancet* **388:**2023-2038.

Tomlinson ES, Maggs JL, Park BK, and Back DJ (1997) Dexamethasone metabolism in vitro: species differences. *J Steroid Biochem Mol Biol* **62:**345-352.

Toribio ML, Gutierrez-Ramos JC, Pezzi L, Marcos MA, and Martinez C (1989) Interleukin-2-dependent autocrine proliferation in T-cell development. *Nature* **342:**82-85.

van den Ouweland FA, Franssen MJ, van de Putte LB, Tan Y, van Ginneken CA, and Gribnau FW (1987) Naproxen pharmacokinetics in patients with rheumatoid arthritis during active polyarticular inflammation. *Br J Clin Pharmacol* **23:**189-193.

van Vollenhoven RF (2009) Sex differences in rheumatoid arthritis: more than meets the eye. *BMC Med* **7:**12.

Vane JR (1971) Inhibition of prostaglandin synthesis as a mechanism of action for aspirin-like drugs. *Nat New Biol* **231:**232-235.

Vrzal R, Stejskalova L, Monostory K, Maurel P, Bachleda P, Pavek P, and Dvorak Z (2009) Dexamethasone controls aryl hydrocarbon receptor (AhR)-mediated CYP1A1 and CYP1A2 expression and activity in primary cultures of human hepatocytes. *Chem Biol Interact* **179:**288-296.

Watson DJ, Rhodes T, Cai B, and Guess HA (2002) Lower risk of thromboembolic cardiovascular events with naproxen among patients with rheumatoid arthritis. *Arch Intern Med* **162:**1105-1110.

Woo S, Pawaskar D, and Jusko WJ (2009) Methods of utilizing baseline values for indirect response models. *J Pharmacokinet Pharmacodyn* **36:**381-405.

Footnotes

We thank the China Scholarship Council for providing the financial support for Xiaonan Li to pursue research at the State University of New York at Buffalo. We thank Donna Ruszaj for technical assistance with LC-MS/MS assay development. This work was funded by the National Institute of General Medical Sciences [Grant GM24211].

Figure Legends

Figure 1. Schematic of the PK/PD/DIS progression model for pharmacokinetics and joint anti-inflammatory effects of DEX and NPX on paw edema in CIA rats. Parameters are defined in the text and in Tables 4 and 5.

Figure 2. Inhibition of Con A-stimulated lymphocyte proliferation by DEX and NPX as single agents (A and B) and in combination (C). Symbols represent experimental data, curves depict fitting of data using Eq. 8. The interaction surface shows model predictions using Eq. 9 based on the fitted parameters listed in Table 2. Red circles identify data above the surface and green circles show data below the surface.

Figure 3. NPX plasma concentration-time profiles in female and male arthritic rats that received 50 mg/kg IP doses of NPX alone (open triangles) or jointly with 0.225 mg/kg SC doses of DEX (solid triangles) and calculated ISF concentrations of total (dashed lines) and unbound (dotted lines) NPX in female and male arthritic rats. Solid curves depict model fittings jointly for all dose groups yielding parameters listed in Table 4.

Figure 4. Total plasma concentration-time profiles of DEX in female and male healthy rats that received 2.25 mg/kg of SC doses of DEX (open circles) and model-simulated total tissue (dashed lines) and unbound ISF concentrations (dotted lines) of DEX in female and male arthritic rats that received 0.225 mg/kg of SC doses of DEX. Solid curves depict model fittings jointly for all healthy animal groups yielding parameters listed in Table 4.

Figure 5. Disease progression of paw edema in female (upper panels) and male (lower panels) arthritic rats after no drug (closed circles), 50 mg/kg of NPX (open circles), 0.225 mg/kg of DEX (open triangles), and the combination of NPX 50 mg/kg and DEX 0.225 mg/kg (open diamonds); time courses of paw volumes in male and female healthy rats (closed triangles). Lines are model fittings of all data jointly yielding parameters listed in Table 5.

Figure 6. Model-simulated paw volume *vs.* time profiles after the administration of different single doses of DEX (0.225, 2.25, 22.5 mg/kg) and the drug combination (NPX 50 mg/kg and DEX 0.225

mg/kg) in female and male arthritic rats. The secondary y-axis indicates percent of baseline (paw volume at peak of edema). The black arrows indicate the time of dosing at 380 h for females and 504 h for males.

DMD Fast Forward. Published on April 17, 2017 as DOI: 10.1124/dmd.117.075614
This article has not been copyedited and formatted. The final version may differ from this version.

TABLE 1

Concentrations of NPX and DEX tested alone and combined in the WBLP assay

Drug	Concentrations in WBLP assay
NPX	0.5, 1, 5, 10, 40, 100, 200, 500, 1000 and 2000 μM
DEX	0.05, 0.1, 0.2, 0.5, 1, 2, 4, 10, 20 and 50 nM
Combinations	DEX (1, 2, 5 and 10 nM) + NPX (50, 100, 150, 200 and 250 μM)

DMD Fast Forward. Published on April 17, 2017 as DOI: 10.1124/dmd.117.075614
This article has not been copyedited and formatted. The final version may differ from this version.

TABLE 2

Parameter estimates for single and combined effects of NPX and DEX on T lymphocyte proliferation

Parameter (units)	Definition	Estimates (CV%)	
		NPX	DEX
I_{max}	Maximum inhibition of cell proliferation	1 (Fixed)	1 (Fixed)
IC_{50} (μg/mL)	Total drug concentration producing 50% of maximal effect	83.97 (1.06)	0.0015 (1.02)
γ	Hill coefficient	2.92 (4.06)	3.04 (1.78)
E_0	Baseline *CPM* in the absence of drug	290453 (2.12)	
Ψ_1	Interaction term for inhibition of cell proliferation	0.94 (2.55)	

DMD Fast Forward. Published on April 17, 2017 as DOI: 10.1124/dmd.117.075614
This article has not been copyedited and formatted. The final version may differ from this version.

TABLE 3

Pharmacokinetic parameters (NCA) based on total plasma concentrations of NPX and DEX following 50 mg/kg IP NPX alone or joint dosing of 0.225 mg/kg SC DEX to arthritic rats and 2.25 mg/kg SC DEX to healthy rats.

Groups	AUC (μg·h/mL)	*CL/F* (mL/h/kg)	*V/F* (mL/kg)	$t_{1/2}$ (h)
NPX (50 mg/kg)				
CIA males (NPX only)	809.8 ± 61.0	61.99 ± 4.87	229.3 ± 48.9	2.55 ± 0.36
CIA males (NPX + DEX)	876.8 ± 77.5	57.39 ± 5.26	198.1 ± 17.6	2.03 ± 0.97
CIA females (NPX only)	936.0 ± 42.2	53.43 ± 2.53	287.1 ± 42.5	3.74 ± 0.64
CIA females (NPX + DEX)	1021.6 ± 118.7	49.45 ± 5.45	192.3 ± 35.8	2.70 ± 0.45
DEX (2.25 mg/kg)				
Healthy males	10.84 ± 0.65	208 ± 12	658 ± 36	2.19 ± 0.12
Healthy females	12.89 ± 2.27	179 ± 35	890 ± 184	3.45 ± 0.11*

*P<0.05 significant difference compared with male healthy group.

DMD Fast Forward. Published on April 17, 2017 as DOI: 10.1124/dmd.117.075614
This article has not been copyedited and formatted. The final version may differ from this version.

TABLE 4

Pharmacokinetic parameter estimates for DEX (2.25 mg/kg SC) and NPX (50 mg/kg IP) in rats

Parameter (units)	Definition	Estimates	CV%
$k_{a,D}$ (1/h)	Absorption rate constant of DEX	2.09	9.33
$f_{d,D}$	Fraction of cardiac plasma flow of DEX	1	Fixed
$CL_{p\ Females}$ (mL/h/kg)	Clearance of DEX in female rats	137.8	3.51
$CL_{p\ Males}$ (mL/h/kg)	Clearance of DEX in male rats	197.7	3.43
K_p	Tissue partition coefficient of DEX	0.63	4.35
V_p (mL/kg)	Plasma volume	32.36 [a]	Fixed
V_t (mL/kg)	Tissue volume	967.6 [a]	Fixed
V_{ISF} (mL/kg)	ISF volume	173.93 [a]	Fixed
Q_{co} (mL/h/kg)	Cardiac plasma flow	7650 [a]	Fixed
$k_{a,N}$ (1/h)	Absorption rate constant of NPX	0.98 [b]	Fixed
$f_{d,N}$	Fraction of cardiac plasma flow of NPX	0.15 [b]	Fixed
CL_{up} (mL/h/kg)	Unbound clearance of NPX in arthritic rats	1438 [b]	Fixed

[a] Physiological parameter values obtained from (Shah and Betts, 2012).
[b] PK parameter values of NPX obtained from (Li et al., 2017b)

TABLE 5

Pharmacodynamic parameter estimates for single and combined effects of DEX and NPX on paw edema in CIA rats

Parameters (units)	Definition	Estimates (CV%)	
		Females	Males
Disease-specific parameters			
t_{onset} (h)	Time of disease onset	258 (0.44)	307 (0.60)
k_{out} (1/h)	Loss of edema rate constant	0.015 (6.07)	0.012 (5.37)
k_{deg} (1/h)	Loss of production rate constant	0.001 (5.98)	0.001 (8.18)
k_g (1/h)	Natural growth rate constant	0.002 (36.0)	0.002 (29.5)
Paw_{ss} (mm^2)	Paw size at steady-state	72.16 (6.64)	103.1 (6.60)
$Paw_{0,ng}$ (mm^2)	Paw size on day 0 for natural growth group	52.7 (2.14)	77.9 (1.53)
$k_{in0,c}$ (mm^2/h)	Disease production rate constant at t_{onset} for control group	2.18 (3.94)	1.72 (4.26)
$Paw_{0,c}$ (mm^2)	Paw size on day 0 for control group	58.8 (1.43)	73.4 (1.58)
$k_{in0,D}$ (mm^2/h)	Disease production rate constant at t_{onset} for DEX treatment	1.93 (4.11)	1.82 (4.27)
$Paw_{0,D}$ (mm^2)	Paw size on day 0 for DEX treatment group	58.9 (1.26)	73.6 (1.42)
$k_{in0,N}$ (mm^2/h)	Disease production rate constant at t_{onset} for NPX treatment	2.06 (4.19)	1.79 (4.39)
$Paw_{0,N}$ (mm^2)	Paw size on day 0 for NPX treatment group	60.0 (1.29)	70.2 (1.55)
$k_{in0,B}$ (mm^2/h)	Disease production rate constant at t_{onset} for combined treatment	2.00 (4.33)	1.80 (4.50)
$Paw_{0,B}$ (mm^2)	Paw size on day 0 for combined treatment group	57.7 (1.28)	74.8 (1.52)
Drug-specific parameters			
$I'_{max,N}$	Maximum inhibition of NPX on production of paw edema	0.75 (Fixed)	1 (Fixed)
$IC'_{50,N}$ (ng/mL)	Unbound ISF concentration of NPX at 50% maximum inhibition	221 (Fixed)	136 (Fixed)
$I'_{max,D}$	Maximum inhibition of DEX on production of paw edema	1 (Fixed)	1 (Fixed)
$IC'_{50,D}$ (ng/mL)	Unbound ISF concentration of DEX at 50% maximum inhibition	0.62 (Fixed)	0.39 (Fixed)
Drug interaction parameter			
Ψ_2	Interaction term for inhibition of paw edema production	1.16 (28.82)	0.98 (37.28)

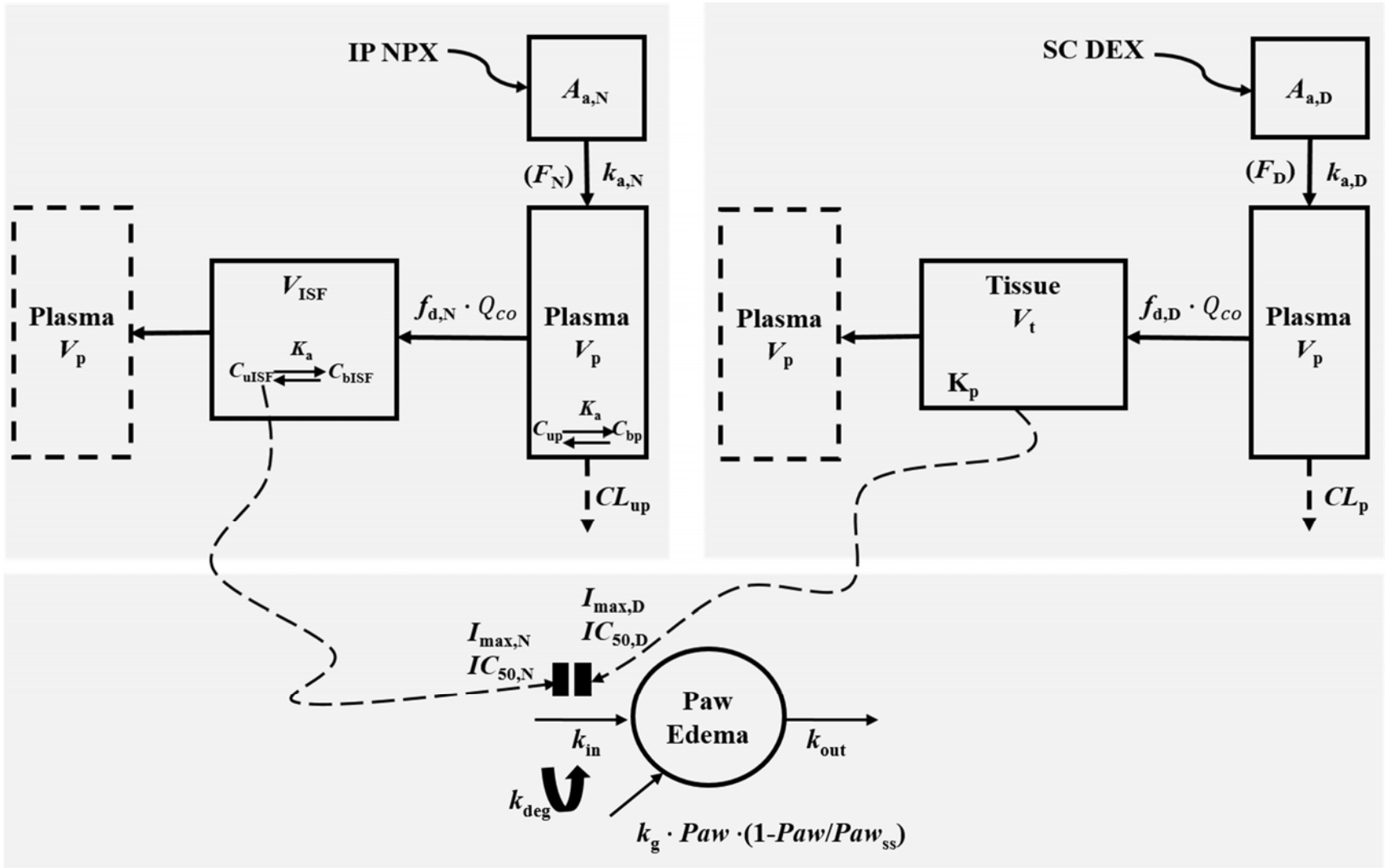

Figure 1

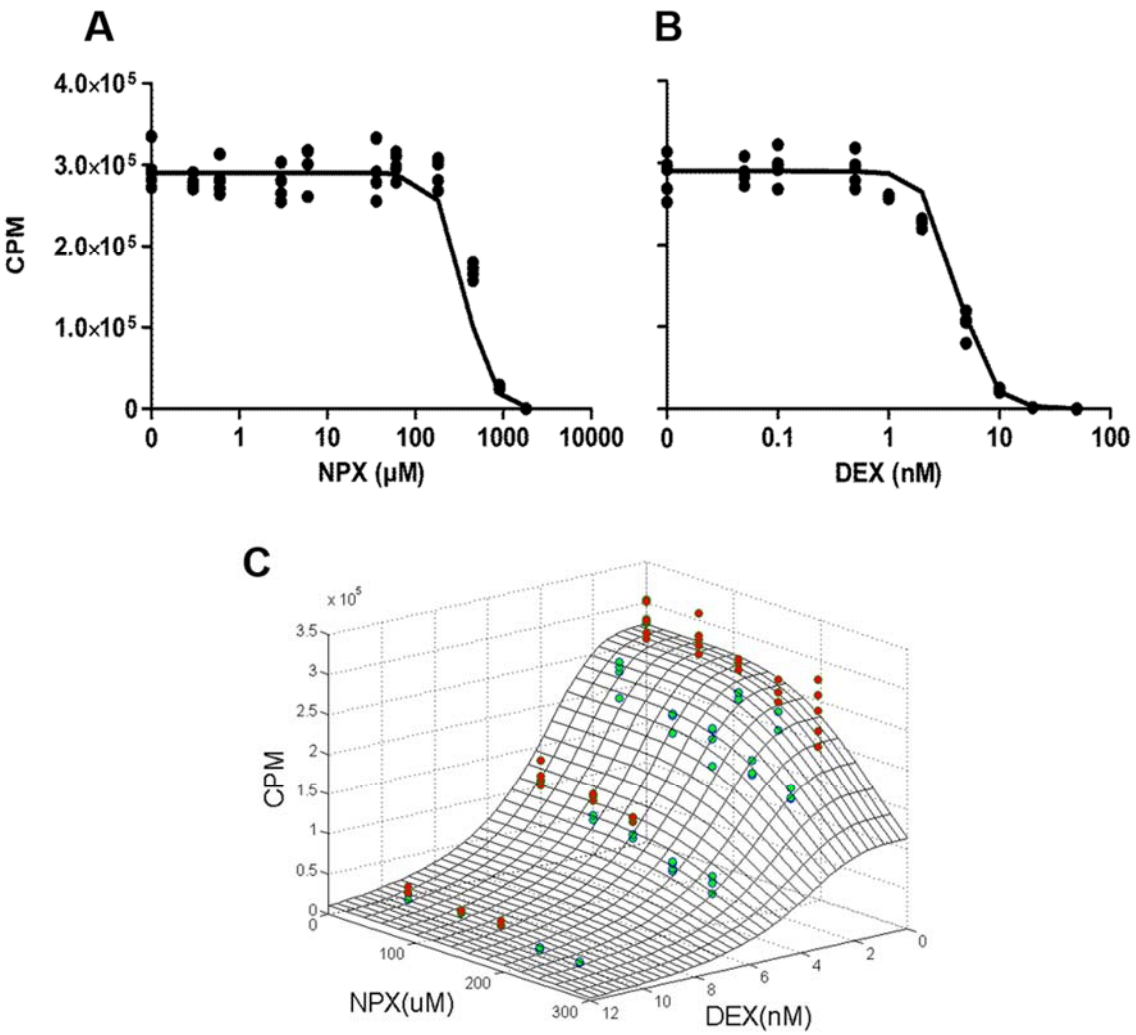

Figure 2

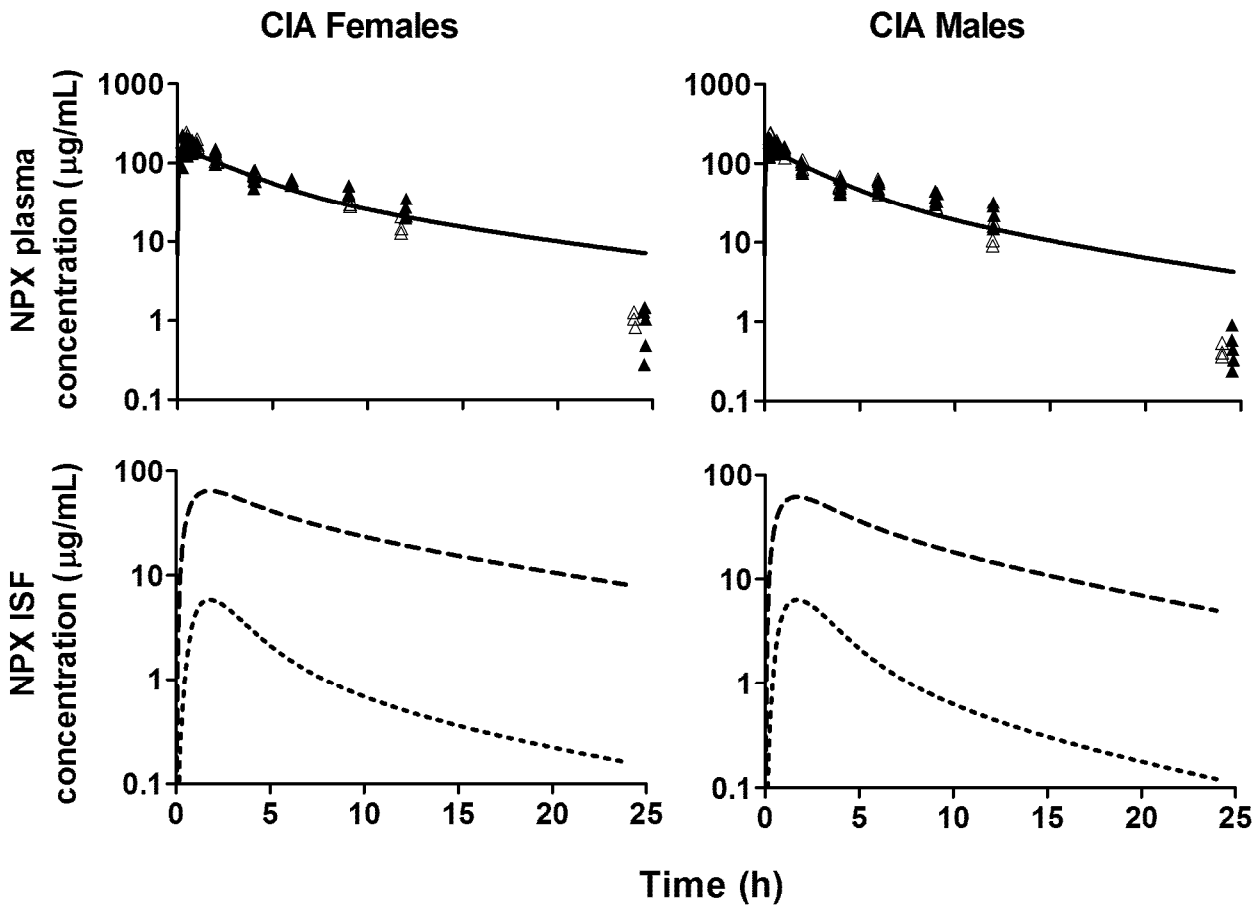

Figure 3

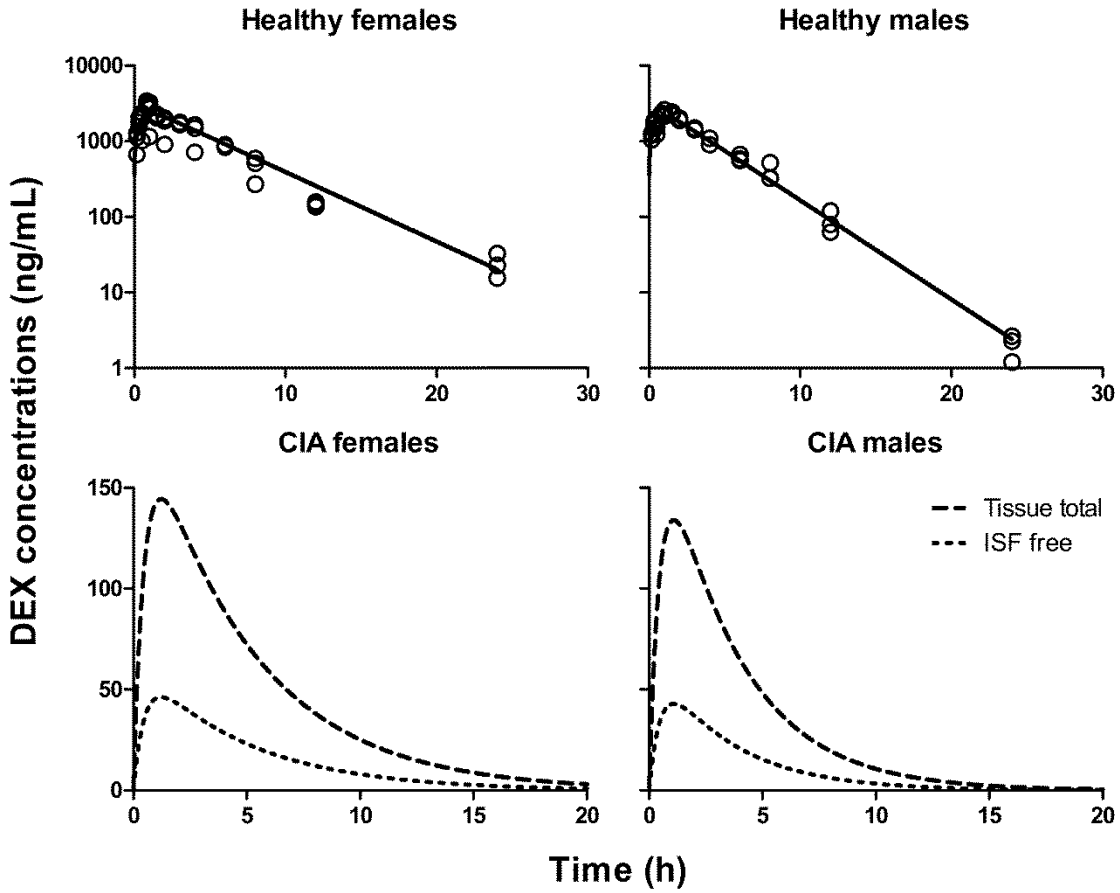

Figure 4

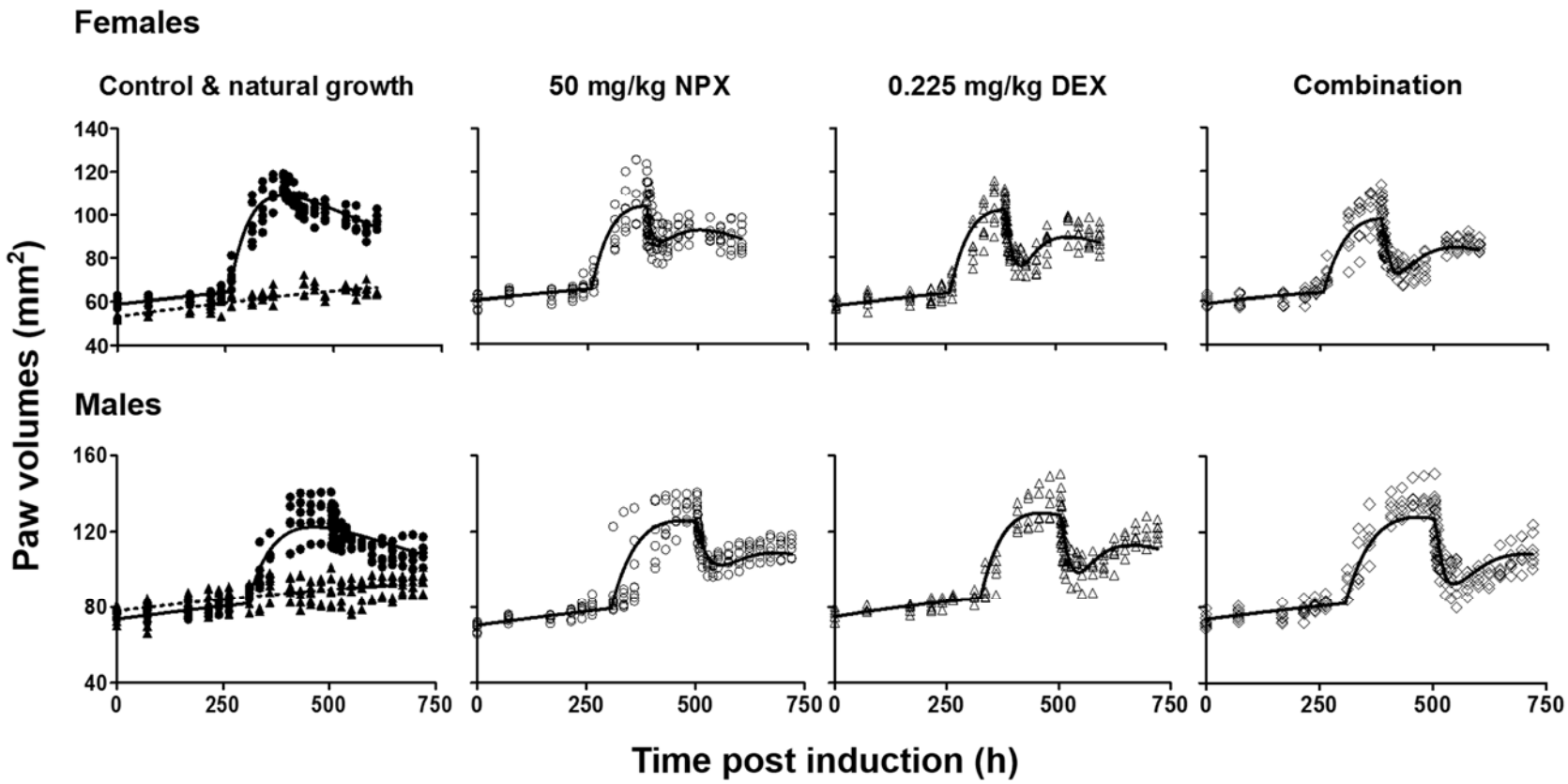

Figure 5

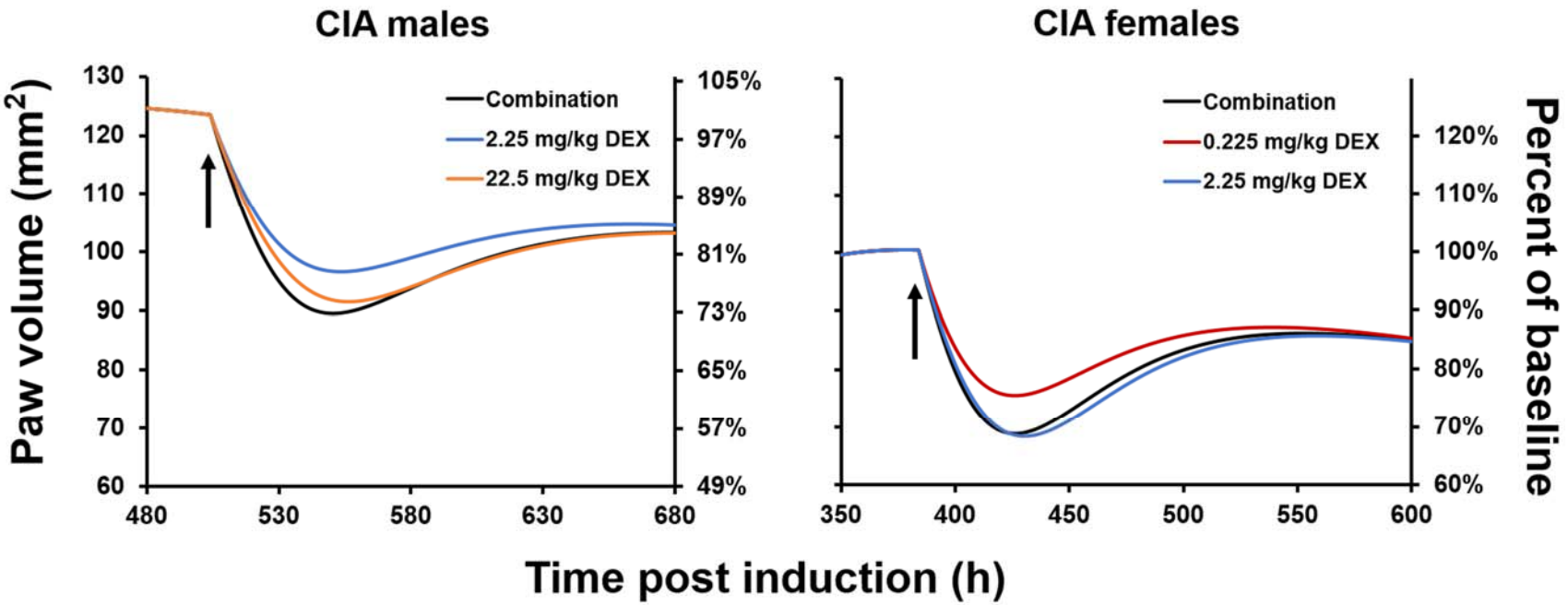

Figure 6